Main Manuscript for

Activity of estrogen receptor beta expressing neurons in the medial amygdala regulates preference towards receptive females in male mice.

Satoshi Takenawa[1], Yutaro Nagasawa[1], Kim Go[1], Yoan Chérasse[2], Seiya Mizuno[3], Kazuhiro Sano[1], and Sonoko Ogawa[1]

[1] Laboratory of Behavioral Neuroendocrinology, University of Tsukuba, Tsukuba, 305-8577, Japan

[2] International Institute for Integrative Sleep Medicine (WPI-IIIS), University of Tsukuba, Tsukuba, Ibaraki 305-8575, Japan.

[3] Laboratory Animal Resource Center and Trans-border Medical Research Center, Institute of Medicine, University of Tsukuba, Tsukuba, Japan.

*Corresponding author

Sonoko Ogawa, Ph.D.

Email : ogawa@neurosci.tsukuba.ac.jp

ORCID : 0000-0003-3976-9987

Author Contributions:

S.T and S.O designed research; S.T, Y.N, K.G, and K.S performed research;

Y.C, and S M provided necessary tools for this research;

S.T, Y.N, and K.G. analyzed data; and S.T. and S.O. wrote the manuscript.

Competing Interest Statement:

No competing interests.

Keywords:

Social behavior, Reproduction, Sexual Preference, Estrogen receptors,

Medial amygdala, Bed nucleus of stria terminalis, Fiber photometry, DREADD, Optogenetics

This PDF file includes:

Main Text

Figures 1 to 5

Abstract

Information processing about sex and reproductive state of conspecific individuals is critical for successful reproduction and survival in males. Generally, male mice exhibit a preference towards sexually receptive (RF) over non-receptive females (XF) or gonadally intact males (IM). Previous studies suggested the involvement of estrogen receptor beta (ERβ) expressed in the medial amygdala (MeA) in male preference towards RF. To further delineate the role played by ERβ in the MeA in the neuronal network regulating male preference, we developed a new ERβ-iCre mouse line with the use of CRISPR-Cas9 system. Fiber-photometry Ca^{2+} imaging revealed that ERβ expressing neurons in the postero-dorsal part of the MeA (MeApd-ERβ^{+} neurons) were more active during social investigation towards RF compared to co-presented XF or IM mice in a preference test. Chemogenetic inhibition of MeApd-ERβ^{+} neuronal activity abolished preference to RF in "*RF vs XF"*, but not "*RF vs IM"*, tests. Analysis with cre-dependent retrograde tracing viral vectors identified the principal part of bed nucleus of stria terminalis (BNSTp) as the projection site of MeApd-ERβ^{+} neurons. Fiber-photometry recording in the BNSTp during preference test revealed that chemogenetic inhibition of MeApd-ERβ^{+} neurons abolished differential neuronal activity of BNSTp cells as well as preference to RF against XF but not against IM mice. Collectively, these findings demonstrate for the first time that MeApd-ERβ^{+} neuronal activity is required for expression of receptivity-based preference (i.e., *RF vs XF*) but not sex-based preference (i.e., *RF vs IM*) in male mice.

Significance Statement

In this study, by introducing a new Cre mice line for ERβ$^+$ cells, we described the function of MeApd-ERβ$^+$ neurons and characteristics of their neuronal activity during preference tests. By fiber photometry and DREADD techniques we found MeApd-ERβ$^+$ neurons have a specific role in receptivity-based (Receptive female vs Non-receptive female) preference but not in sex-based (Receptive female vs Intact Male) preference in male mice. We also described this specific role of MeApd-ERβ$^+$ neurons is achieved by regulating the neuronal activity of downstream BNSTp neurons during the receptivity-based preference, but not in sex-based preference. Our findings contribute to a better understating of the function of estrogen receptor expressing neurons in the neuronal network for the male-type reproductive behaviors.

Main Text

Introduction

Information processing about sex and reproductive state of conspecific individuals is critical for successful reproduction and survival in males. Male rats and mice primarily use olfactory cues to discriminate and find the right individual for efficient expression of sexual behavior. In general, males show a preference for receptive females over non-receptive females or males. During a preference test with a pair of 'stimulus' animals, they spend more time investigating females over males, and females in estrus over non-estrus states (1–4). Since preference towards sexually receptive females is disrupted by castration, action of gonadal steroid hormones is critical (1, 3, 5, 6).

Olfactory information about sex and reproductive state is initially processed in the main and accessory olfactory bulbs (MOB/AOB) under influence of gonadal steroids (7–11). The information is further processed in the amygdala for expression of preference. Lesions of the amygdala alter preference towards females over males in male rodents (12–15). Among various subregions of the amygdala, the medial amygdala (MeA) plays a central role for olfactory information processing which leads to adaptive expression of reproductive behaviors (9, 16–18). Neurons in the MeA, particularly those in the posteroventral (MeApv) and posterodorsal (MeApd) subdivisions, project to various brain areas, such as the bed nucleus of the stria terminalis (BNST) and ventromedial nucleus of the hypothalamus (VMH), which are involved in the expression of sexual and aggressive behaviors (19–21). Furthermore, the existence of distinctive neuronal sub-populations within the MeA that specifically respond to certain olfactory cues such as males, females, or pups, has been reported (22, 23).

It is well established that testosterone regulates the expression of male type social behavior by acting not only on androgen receptors but also on estrogen receptors (ER), ERα and ERβ, after being converted to estradiol in the brain. In the MeA, both ERα and ERβ, as well as aromatase which converts testosterone to estradiol are widely expressed (24–31). Previous

studies with RNAi-mediated brain site-specific knockdown in adult male mice revealed that neither type of ER in the MeA is required for the expression of sexual or aggressive behavior (4, 32). However, the presence of ERβ in the MeA was necessary for male mice to show preference towards receptive females. Importantly, the disruption of behavioral phenotype induced by ERβ silencing in the MeA was only seen when male mice were tested for preference between a receptive female (RF) mouse and a non-receptive female (XF) mouse, but not when they were tested for preference between an RF mouse and a gonadally intact male (IM) mouse (4). Collectively, these studies indicate that the ERβ expressing neurons in the MeA regulates "receptivity-based preference" (i.e., RF over XF) but not "sex-based preference" (i.e., RF over IM) in male mice. However, the exact mechanism, particularly whether and how neuronal activity of ERβ expressing neurons in the MeA is involved in this regulation, is not known to this date.

To address this question, we first generated a transgenic mouse line in which improved Cre (*iCre*) was knocked-in just before the stop codon of endogenous ERβ gene (*Esr2*) thus allowing us to target ERβ-expressing cells specifically with adeno-associated virus (AAV)-mediated gene delivery. Using this ERβ-iCre mouse line, we recorded neuronal activity of ERβ positive neurons during preference tests in the postero-dorsal part of the MeA (MeApd) where ERβ positive neurons are mainly localized (33). We then examined whether manipulation of MeApd-ERβ$^+$ neuronal activity with the use of optogenetic and chemogenetic methods alter the preference of male mice. In addition, we examined the effect of chemogenetic inhibition of MeApd-ERβ$^+$ neurons on receptivity-based and sex-based preference as well as on neuronal activity of the BNST, as a primary downstream brain region of the MeA.

Results

(Study 1）Fiber photometry recording of MeApd-ERβ$^+$ neuronal activity during preference tests

We first examined neuronal activity of MeApd-ERβ$^+$ neurons in freely behaving mice during a 10 min preference test. Newly generated ERβ-iCre male mice were injected with a Cre

dependent genetically encoded Ca^{2+} sensor GCaMP7f in the MeApd and subjected to fiber photometry recordings (Fig.1A, B) in the preference test setup (Fig.1C).

During receptivity-based preference tests with *RF vs XF* stimuli, male mice showed preference towards RF, as well as higher neuronal activity of MeApd-ERβ^{+} neurons during RF investigation. Male mice stayed much longer time (Student's t-test n=7, t =5.428 df=6 p=0.0008***; Fig. 1D) and showed longer duration of sniffing (Student's t-test n=7, t =5.428 df=6 p =0.0008***; Fig. 1E) in the contact area with RF than with XF, suggesting a preference towards RF mice. Analysis of fiber photometry recordings revealed that changes of MeApd-ERβ^{+} GCaMP7f signals starting at the onset of sniffing behavior (Fig.1F) were clearly different between RF and XF stimuli. Further statistical analysis of neuronal activity of the entire 8 sec (Student's t-test, n = 7, t = 8.293 df = 6 p<0.0001***; Fig.1G) confirmed peak value was significantly higher during sniffing towards RF than XF.

In sex-based preference tests with "*RF vs IM"* stimuli, male mice demonstrated a preference towards RF. This was also accompanied with higher MeApd-ERβ^{+} neuronal activity during RF, compared to IM, investigation, similar to the observation found during "*RF vs XF"* test. Male mice tended to spend longer time (Student's t-test, n = 7, t = 1.874 df = 6 p = 0.0550; Fig.1H) and showed longer duration of sniffing (Student's t-test, n = 7, t = 3.591 df = 6 p = 0.0057***; Fig.1I) in the contact area with RF than with IM, suggesting a preference towards RF mice. Fiber photometry recordings revealed that changes of MeApd-ERβ^{+} GCaMP7f signals during RF sniffing were different from those of IM (Fig.1J). Peak values of neuronal activity during 8 sec were higher during sniffing towards RF than IM (Student's t-test, n = 7, t = 3.114 df = 6 p = 0.0104*; Fig.1K).

(Study 2) Responses of MeApd-ERβ^{+} neurons toward individually presented social stimuli

In the study 1, we demonstrated that MeApd-ERβ^{+} neurons in male mice were activated with a higher probability during sniffing of RF mice compared to sniffing of "co-presented" XF or IM mice. From there results, we could assume two possibilities, i.e., these MeApd-ERβ^{+} neurons are

specifically responding to receptive females, or simply responding toward preferred amimals. Hence, to further understand the function of MeApd-ERβ$^+$ neurons, we examined how these neurons respond to stimulus (RF, XF and IM) presented individually.

In the analysis of activity of MeApd-ERβ$^+$ neurons during preference tests for *RF vs empty*, male mice tended to show longer time spent in the RF contact area compared to an empty cylinder area (Student's t-test n=5, t =2.009 df=4 p =0.0576; Fig.2A). GCaMP7f signal patterns were different between RF and empty (Fig.2B) and peak GCaMP7f signals were much higher during sniffing of RF compared to sniffing an empty cylinder (Student's t-test n=5, t =3.511 df=4 p =0.0123*; Fig.2C).

In *XF vs empty* tests, we found that male mice demonstrated longer time spent in the contact area of XF compared to an empty cylinder (Student's t-test n=5, t =3.480 df=4 p =0.0127*; Fig.2D). In parallel with behavioral events, activity patterns (Fig.2E) and peak (Student's t-test n=5, t =1.576 df=4 p =0.0951; Fig.2F) of GCaMP7f signals tended to be different between sniffing of XF and empty cylinders.

Similarly, in *IM vs empty* preference tests, we found that male mice spent longer time in the contact area of IM (Student's t-test n=5, t =8.642 df=4 p =0.0005***; Fig.2G), accompanied with higher neuronal activity during sniffing toward IM compared to an empty cylinder (Fig.2H, 2I, Student's t-test n=5, t =3.516 df=4 p =0.0123* for Fig.2P).

(Study 3) DREADD inhibition of MeApd-ERβ$^+$ neurons disrupt the expression of "*RF vs XF*", but not "*RF vs IM*", preference

To further investigate whether MeApd-ERβ$^+$ neurons actually play a role in the expression of preference, we chemogenetically inhibited MeApd-ERβ$^+$ neuronal activity and examined the effects on sniffing behavior during preference tests or this purpose, a Cre dependent inhibitory DREADD expressing virus or control virus was bilaterally injected to the MeApd in ERβ-iCre mice (Fig. 3A, 3B). In each male mouse, effects of silencing of MeApd-ERβ$^+$ neurons on preference were examined for both "*RF vs XF*" and "*RF vs IM*" preference tests (Fig. 3C).

In "*RF vs XF"* tests, we found the inhibition of MeApd-ERβ$^+$ neurons by Clozapine-N-oxide (CNO) administration (drug) did not affect total moving distance (Fig.S2A) but clearly reduced duration of time spent in RF contact area (Fig. 3D) and sniffing towards RF cylinder (Fig. S2B). The ratio of time spent in RF contact area against total duration was not significantly different from chance levels (Repeated measures ANOVA, drug x virus $F_{(2,36)} = 7.244$ $p = 0.0023$***; Fig.3D), indicating abolishment of preference. In contrast to effects seen in "*RF vs XF"* tests, inhibition of MeApd-ERβ$^+$ neuronal activity did not affect any behavioral measures in "*RF vs IM"* test (Fig. 3E, S2C, S2D).

(Study 4) Role of MeApd-ERβ$^+$ in neuronal network involved in receptivity-based preference

In the Study 1, MeApd-ERβ$^+$ neurons showed increased activity during sniffing towards RF in both "*RF vs XF"* and "*RF vs IM"* preference tests. However, chemogenetic inhibition of MeApd-ERβ$^+$ neuronal activity in the Study 3 affected expression of RF-directed preference only against XF, but not against IM. Based on these findings, we hypothesized that neuronal networks being activated during receptivity-based and sex-based preference tests may be different. To test this, we first identified projection patterns of MeApd-ERβ$^+$ neurons by injecting Cre dependent anterograde viral tracer. We found robust projections of MeApd-ERβ$^+$ neurons to the bed nucleus of the stria terminalis (BNST), particularly the principal region (BNSTp) (Fig.S3A-C)

Then to examine the effects of chemogenetic inhibition of MeApd-ERβ$^+$ on neuronal activity of BNSTp neurons, we bilaterally injected a Cre dependent inhibitory DREADD expressing virus to target MeApd-ERβ$^+$ neurons and unilaterally injected a non-specific GCaMP7f expressing viral vector in the BNSTp for recording BNSTp neuronal activity (Fig.4A-C). Mice were tested four times as shown in Fig.S4A. In "*RF vs XF"* test, preference towards RF was disrupted in CNO (drug) injected tests, as expected (Fig.S4B). Similar to MeApd-ERβ$^+$ neurons, BNSTp neurons demonstrated higher neuronal activity towards RF during "*RF vs XF"* preference tests with saline injection (i.e., without inhibition of MeApd-ERβ$^+$ neurons; Fig.4D). When we inhibited the MeApd-

ERβ$^+$ neurons with CNO injection, neuronal activity of downstream BNSTp neurons was not different between RF and XF sniffing events (Fig. 4E). This was in paralel with the behavioral effect of DREADD inhibition of MeApd-ERβ$^+$ neurons (shown in Fig. S4B). During preference tests with CNO, changes of BNSTp GCaMP7f signals (Fig.4E) and peak values (Repeated measures ANOVA, drug x stimulus $F_{(1,20)} = 23.80$ $p < 0.0001$***; post-hoc Bonferroni's test (RF-XF x drug); Saline: p<0.0007***, CNO: *p* value>0.9999 Fig.4F) were no longer different between RF sniffing and XF sniffing events.

In contrast, inhibition of MeApd-ERβ$^+$ neurons did not affect preference in "*RF vs IM"* tests, as expected based on the findings in the Study 3. Mice spent longer time in RF contact area than IM contact area in both saline and CNO injection conditions (Fig.S4E). In parallel, DREADD inhibition of MeApd-ERβ$^+$ neurons did not affect BNSTp GCaMP7f signals. In both saline and CNO conditions, changes of BNSTp GCaMP7f signals (Fig.4G for saline, Fig. 4H for CNO) and peak values (Repeated measures ANOVA, drug x stimulus $F_{(1,20)} = 0.3787$ $p = 0.5452$ *ns*; Fig.4I) were different between RF sniffing and IM sniffing events.

Discussion

In this study, we investigated possible neuronal mechanisms controlling sexual preference in male mice by focusing on neuronal activity of MeApd-ERβ$^+$ cells. In our previous gene silencing study with the use of RNAi methods, we have demonstrated gene expression of ERβ in the MeA is essential for males' preference towards RF over XF, but not over IM, mice(4). The present study demonstrates that not only gene expression of ERβ but also neuronal excitation of ERβ expressing cells, particularly in the MeApd, is critical for receptivity-based (*RF vs XF*) preference but not sex-based (*RF vs IM*) preference. Although a number of previous studies, in mice and rats, suggested that testosterone is necessary for males to show preference towards RF over XF as well as IM stimuli (1, 3, 6), the exact mechanism of action has not been determined. Our findings provide an important piece of evidence for understanding of ERβ-mediated gonadal steroid action and it's expressing neurons in the regulation of male sexual preference.

MeApd-ERβ$^+$ neurons were activated in response to sniffing of receptive females

In the fiber-photometry recordings, we found the neuronal activity of MeApd ERβ$^+$ neurons increased their activity during RF investigation in "*RF vs XF"* preference tests in parallel with their overall higher sniffing behavior towards RF (Study 1, Fig. 1). Likewise, higher neuronal activity of MeApd-ERβ$^+$ neurons was seen during investigation of RF in "*RF vs IM"* tests, suggesting that activity of MeApd-ERβ$^+$ neurons may be related to males' behavioral preference towards RF in both "*RF vs XF"* and "*RF vs IM"* tests. However, when stimulus mice were presented individually, similer patterns of MeApd-ERβ$^+$ activity were detected during sniffing of all three types of stimuli, i.e., RF, XF and IM (Study 2, Fig. 2). These findings suggest that MeApd-ERβ$^+$ neurons can be similarly excited by sniffing of RF, XF and IM, but they become distinctively more active during sniffing of RFs presented as a pair with XF or IM.

In the MeA, existence of distinctive neuronal sub-populations which respond to a specific type of stimulus, such as males, females, or pups, was previously reported(22). However, in the previous reports, each type of stimuli was presented individually. The present study, on the other hand, revealed unique characteristics of MeApd-ERβ$^+$ neurons which respond differently depending on how the stimuli are presented. We conclude that activity of MeApd-ERβ$^+$ neurons is not specific to a particular type of stimuli but rather underlies a preference to a specific stimulus (i.e., RF) over others (i.e., XF or IM). This notion is further supported by additional optogenetical studies (see Fig.S4). By optogenetically stimulating the MeApd-ERβ$^+$ neurons when males started sniffing a XF mouse in "*RF vs XF"* preference tests, we could successfully switch their preference from RF to originally less preferred XF. These findings show artificial activation of MeApd-ERβ$^+$ neurons can promote further sniffing to that specific stimulus (see Fig.S4H).

Inhibition of MeA ERβ$^+$ neuronal activity abolished receptivity-based preference (*RF vs XF*) but not sex-based preference (*RF vs IM*) in male mice.

Although we found MeApd-ERβ$^+$ neurons were distinctly more active during sniffing of RFs in

both "*RF vs XF"* and "*RF vs IM"* preference tests, the effects of chemogenetic silencing of MeApd-ERβ$^+$ neuronal activity on males' preference behavior were different between the two types of tests (Study 3, Fig. 3). Preferential sniffing towards RF over XF was completely abolished by CNO injection in the hM4Di injected group. On the other hand, males kept showing more sniffing towards RF over IM even when MeApd-ERβ$^+$ neurons were not activated. These findings suggest that although MeApd-ERβ$^+$ neurons are active during investigation of receptive female mice, regardless of the type of preference tests, actual activation is only necessary for preference based on differences for receptivity but not for sex.

These results are along the same line with a previous brain site-specific ERβ silencing study. Knockdown of ERβ gene expression in the MeA abolished receptivity-based preference but not sex-based preference(4). Therefore, not just the expression of ERβ, but the actual neuronal activation of MeApd-ERβ$^+$ neurons is necessary for receptivity-based preference in male mice.

ERβ knockdown may induce not only a lack of ERβ gene expression but also a decrease of neuronal activity among MeApd-ERβ$^+$ neurons partly through rapid nongenomic action via ERβ. Several reports have demonstrated that membrane bound ERβ can modulate neuronal activity directly under the existence of 17β-estradiol, independent from their genomic action(35–37) .

BNSTp, as a primary projection site of MeApd-ERβ$^+$ neurons, were activated during sniffing of receptive females in both receptivity-based and sex-based preference tests.

Lack of effects of chemogenetic inhibition of MeApd-ERβ$^+$ neuronal activity on sex-based preference led us to hypothesize that differences in mechanisms between receptivity-based and sex-based preference may be at downstream projection site(s) of MeApd-ERβ$^+$ neurons. With the use of mice generated by mating of ERβ-iCre and ERβ-RFP mice, we found that the majority of MeApd-ERβ$^+$ neurons project to the BNSTp (see, Fig.S5A-C). The distinct projection pattern of MeApd-ERβ$^+$ neurons led us to further delineate the role of neuronal circuit consisting of MeApd-ERβ$^+$ and BNSTp in the regulation of receptivity-based and sex-based preference. Our fiber photometry recordings within the BNSTp revealed higher neuronal activity during RF investigation

and higher probability to be active around RF cylinder in both "*RF vs XF*" and "*RF vs IM*" preference tests (Study 4, Fig. 4). This is similar to what we found in fiber photometry recordings of MeApd-ERβ$^+$ neurons (Study 1, Fig. 1). Also, similar to the MeA, a number of previous studies reported that neurons in the BNSTp form a network for male social behavior, that respond to a specific type of stimuli presented individually(7, 8, 38, 18, 39). To this extent, our findings are the first clear demonstration of differential neuronal response of BNSTp during investigation of RF co-presented with XF or IM mice.

Differential role of the MeApd-ERβ$^+$ and BNSTp neuronal circuit in receptivity-based and sex-based preference of male mice

By inhibiting the MeApd-ERβ$^+$ neurons during the BNSTp recordings, we aimed to determine the role of functional connectivity between MeApd-ERβ$^+$ neurons and BNSTp in receptivity-based and sex-based preference of male mice (Study 4, Fig. 4). As expected, silencing of the MeApd-ERβ$^+$ neurons abolished preference towards RF during "*RF vs XF"* preference test. In parallel with this, BNSTp neuronal activity was influenced by silencing of MeApd-ERβ$^+$ neurons. Levels of neuronal activity and probability of activation around presented cues were no longer different between RF and XF. In contrast, in "*RF vs IM"* preference tests, silencing of the MeApd-ERβ$^+$ neurons did not affect differential BNSTp neuronal excitation during RF and IM sniffing as well as preferential behavior towards RF over IM. These results suggest inputs from MeApd-ERβ$^+$ neurons to BNSTp are only necessary for receptivity-based and not for sex-based preference.

In summary, this study demonstrated, for the first time, MeApd-ERβ$^+$ neuronal activity is essential in the regulation of receptivity-based, but not sex-based, preference in male mice (Fig. 5 Summary schematics). This functional specificity of MeApd-ERβ$^+$ neurons is exerted by influencing activity of downstream BNSTp neurons. In conclusion, our finding demonstrating that MeApd-ERβ$^+$ neuronal activity is required for expression of receptivity-based, but not sex-based,

preference. This contributes to a better understating of mechanisms of action of gonadal steroids on the neuronal network regulating the expression of male-type reproductive behaviors.

Materials and Methods

Animals

ERβ-iCre mice were generated by CRISPR-Cas9 system described previously (see SI and Fig.S6 for details) (40). Male ERβ-iCre positive mice with C57BL/6N background, 10- to 14-week-old at beginning of each study, were used as experimental animals. 10- to 18-week-old male and female ERβ-iCre negative mice were used as stimulus animals for preference behavioral tests. All mice were housed in 12h-12h light-dark cycle (lights off at noon) with food and water available *ad libitum*. All experiments were approved by the Animal Care and Use Committee and the Recombinant DNA Use Committee at the University of Tsukuba and conducted under the National Institute of Health guidelines. All efforts were made to minimize the number of animals used and their suffering. All experimental subjects were stereotaxically injected with various types of viruses under inhalation anesthesia with 1-3% isoflurane (Pfizer). All viruses used in this study is listed in Table S2.

Preference test

Preference test apparatus and paradigm were designed based on previous studies from our laboratory(4, 41). Briefly, each experimental mouse was placed in a white plastic open field (33cm × 28cm) under red or dim light (10lux) for 10min. Animals used as stimuli were individually placed in a transparent acrylic quarter cylinder (7cm base radius) with 13 small holes (Φ7 mm) on the rounded side.Time spent in the contact area, which was defined as area 8 cm from the outer surface of the cylinders, and cumulative number and duration of sniffing behavior defined as nose touch at perforated parts of the cylinders, were recorded. Detailed information for all experimental

procedure is available in supplemental methods.

Fiber photometry recording during preference tests.

ERβ-iCre positive mice were stereotaxically injected with either 600nl of AAV9-hSyn-DIO-GCaMP7f at MeApd for Study 1 and 2, or non-specific AAV9-hSyn-GCaMP7f at the BNSTp for Study 4. One week after virus injection, a NA.039, Φ230μm glass optic fiber (RWD Life Science) was inserted 200μm above the injection site. Fiber photometry recordings were done during preference tests under red light with the use of the DORIC fiber photometry system (DORIC Lenses). 465 nm LED light was used for excitation of GCaMP7f, and 525 nm emission light was filtered for recording.

All Fiber photometry recordings were analyzed based on mouse sniffing behavior. Two seconds before and 8 s from sniffing onset was extracted from the image data. These data were converted to dF/F0 (dF = 8 s from sniffing onset, F0 = mean signals from 2 s before sniffing onset) and then normalized into Z score. We determined the highest signals within 8 s window as peak signals and mean peak signal was derived for each stimulus. Processed fiber photometry data was analyzed and aligned with animal behavioral annotation derived by BORIS (42) and Deeplabcut (43) data by python (ver. 3.8.1).

Chemogenetic manipulation of MeApd-ERβ$^+$ neurons

ERβ-iCre positive mice were injected stereotaxically with either 300μl of AAV2-hSyn-DIO-hM4Di-mCherry or AAV2-hSyn-DIO-mCherry control virus at the MeApd. They were subjected for investigation of chemogenetic inhibition of MeApd- ERβ$^+$ neuronal activity on preference behavior in male mice, as either simple behavioural analysis (Study 3) or combined analysis with fiber photometry recording in the BNSTp (Study 4). On the test day, animals were injected by i.p with either saline or clozapine n-oxide dihydrochloride (CNO; Sigma-Aldrich) at a dose of 1mg/kg BW 15min prior to test.

Statistical analysis

All data was statistically analyzed by student's t-test or ANOVA with GraphPad Prism9. Significant differences were considered at $p < 0.05$*, $p < 0.01$**, $p < 0.001$*** , $p < 0.0001$**** . All statistical analysis used, and details are summarized in TableS3.

Acknowledgments

The authors thank Dr. C. Pavlides for critical reading of the manuscript. We also thank prof. Aki Takahashi for allowing us to use her equipment. Y. Asano and A. Sagehashi for their technical and secretarial assistance. This work was supported by grant-in-aid for Scientific Research 15H05724 and 22H02941 to SO.

References

1. E. Rose, L. C. Drickamer, Castration, sexual experience, and female urine odor preferences in adult BDF1 male mice. *Bull. Psychon. Soc.* **5**, 84–86 (1975).
2. M. de Bruijn, M. Broekman, P. van der Schoot, Sexual interactions between estrous female rats and castrated male rats treated with testosterone propionate or estradiol benzoate. *Physiol. Behav.* **43**, 35–39 (1988).
3. K. Xiao, Y. Kondo, Y. Sakuma, Sex-specific effects of gonadal steroids on conspecific odor preference in the rat. *Horm. Behav.* **46**, 356–361 (2004).
4. M. Nakata, *et al.*, Effects of Prepubertal or Adult Site-Specific Knockdown of Estrogen Receptor β in the Medial Preoptic Area and Medial Amygdala on Social Behaviors in Male Mice. *eNeuro* **3**, ENEURO.0155-15.2016 (2016).
5. S. Dhungel, S. Urakawa, Y. Kondo, Y. Sakuma, Olfactory preference in the male rat depends on multiple chemosensory inputs converging on the preoptic area. *Horm. Behav.* **59**, 193–199 (2011).
6. Y. Kondo, H. Hayashi, Neural and Hormonal Basis of Opposite-Sex Preference by Chemosensory Signals. *Int. J. Mol. Sci.* **22**, 8311 (2021).
7. J. Bakker, M. J. Baum, A. K. Slob, Neonatal inhibition of brain estrogen synthesis alters adult neural Fos responses to mating and pheromonal stimulation in the male rat. *Neuroscience* **74**, 251–260 (1996).
8. J. M. Fiber, J. M. Swann, Testosterone differentially influences sex-specific pheromone-stimulated Fos expression in limbic regions of Syrian hamsters. *Horm. Behav.* **30**, 455–473 (1996).
9. K. L. Martel, M. J. Baum, A centrifugal pathway to the mouse accessory olfactory bulb from the medial amygdala conveys gender-specific volatile pheromonal signals. *Eur. J. Neurosci.* **29**, 368–376 (2009).

10. M. Yoshikage, I. Toshiaki, K. Seiichi, K. Nobuo, M. Nishimura, Sex steroids modulate the signals from volatile female odors in the accessory olfactory bulb of male mice. *Neurosci. Lett.* **413**, 11–15 (2007).

11. T. Inbar, R. Davis, J. F. Bergan, A sex-specific feedback projection from aromatase-expressing neurons in the medial amygdala to the accessory olfactory bulb. *J. Comp. Neurol.* **530**, 648–655 (2022).

12. Y. Kondo, Lesions of the medial amygdala produce severe impairment of copulatory behavior in sexually inexperienced male rats. *Physiol. Behav.* **51**, 939–943 (1992).

13. Y. Kondo, B. D. Sachs, Disparate effects of small medial amygdala lesions on noncontact erection, copulation, and partner preference. *Physiol. Behav.* **76**, 443–447 (2002).

14. P. M. Maras, A. Petrulis, Chemosensory and steroid-responsive regions of the medial amygdala regulate distinct aspects of opposite-sex odor preference in male Syrian hamsters. *Eur. J. Neurosci.* **24**, 3541–3552 (2006).

15. A. Petrulis, Neural mechanisms of individual and sexual recognition in Syrian hamsters (Mesocricetus auratus). *Behav. Brain Res.* **200**, 260–267 (2009).

16. M. J. Baum, Sexual differentiation of pheromone processing: Links to male-typical mating behavior and partner preference. *Horm. Behav.* **55**, 579–588 (2009).

17. K. Hashikawa, Y. Hashikawa, A. Falkner, D. Lin, The neural circuits of mating and fighting in male mice. *Curr. Opin. Neurobiol.* **38**, 27–37 (2016).

18. D. W. Bayless, N. M. Shah, Genetic dissection of neural circuits underlying sexually dimorphic social behaviours. *Philos. Trans. R. Soc. Lond. B. Biol. Sci.* **371**, 20150109 (2016).

19. N. S. Canteras, R. B. Simerly, L. W. Swanson, Organization of projections from the medial nucleus of the amygdala: A PHAL study in the rat. *J. Comp. Neurol.* **360**, 213–245 (1995).

20. H.-W. Dong, G. D. Petrovich, L. W. Swanson, Topography of projections from amygdala to bed nuclei of the stria terminalis. *Brain Res. Rev.* **38**, 192–246 (2001).

21. D. J. Anderson, Optogenetics, Sex, and Violence in the Brain: Implications for Psychiatry. *Biol. Psychiatry* **71**, 1081–1089 (2012).

22. Y. Li, *et al.*, Neuronal Representation of Social Information in the Medial Amygdala of Awake Behaving Mice. *Cell* **171**, 1176-1190.e17 (2017).

23. S. Yao, J. Bergan, A. Lanjuin, C. Dulac, Oxytocin signaling in the medial amygdala is required for sex discrimination of social cues. *eLife* **6**, e31373 (2017).

24. A. Foidart, N. Harada, J. Balthazart, Aromatase-immunoreactive cells are present in mouse brain areas that are known to express high levels of aromatase activity. *Cell Tissue Res.* **280**, 561–574 (1995).

25. P. J. Shughrue, M. V. Lane, I. Merchenthaler, Comparative distribution of estrogen receptor-α and -β mRNA in the rat central nervous system. *J. Comp. Neurol.* **388**, 507–525 (1997).

26. P. Shughrue, P. Scrimo, M. Lane, R. Askew, I. Merchenthaler, The Distribution of Estrogen Receptor-β mRNA in Forebrain Regions of the Estrogen Receptor-α Knockout Mouse. *Endocrinology* **138**, 5649–5652 (1997).

27. S. Ogawa, *et al.*, Survival of reproductive behaviors in estrogen receptor β gene-deficient (βERKO) male and female mice. *Proc. Natl. Acad. Sci.* **96**, 12887–12892 (1999).

28. S. W. Mitra, *et al.*, Immunolocalization of Estrogen Receptor β in the Mouse Brain: Comparison with Estrogen Receptor α. *Endocrinology* **144**, 2055–2067 (2003).

29. S. Ogawa, *et al.*, Abolition of male sexual behaviors in mice lacking estrogen receptors α and β (αβERKO). *Proc. Natl. Acad. Sci.* **97**, 14737–14741 (2000).

30. R. J. Handa, S. Ogawa, J. M. Wang, A. E. Herbison, Roles for Oestrogen Receptor β in Adult Brain Function. *J. Neuroendocrinol.* **24**, 160–173 (2012).

31. K. Sano, *et al.*, Pubertal activation of estrogen receptor α in the medial amygdala is essential for the full expression of male social behavior in mice. *Proc. Natl. Acad. Sci.* **113**, 7632–7637 (2016).

32. K. Sano, M. C. Tsuda, S. Musatov, T. Sakamoto, S. Ogawa, Differential effects of site-specific knockdown of estrogen receptor α in the medial amygdala, medial pre-optic area, and ventromedial nucleus of the hypothalamus on sexual and aggressive behavior of male mice. *Eur. J. Neurosci.* **37**, 1308–1319 (2013).

33. S. Sagoshi, *et al.*, Detection and Characterization of Estrogen Receptor Beta Expression in the Brain with Newly Developed Transgenic Mice. *Neuroscience* **438**, 182–197 (2020).

34. B. L. Roth, DREADDs for Neuroscientists. *Neuron* **89**, 683–694 (2016).

35. M. Wong, R. L. Moss, Long-term and short-term electrophysiological effects of estrogen on the synaptic properties of hippocampal CA1 neurons. *J. Neurosci.* **12**, 3217–3225 (1992).

36. T. Smejkalova, C. S. Woolley, Estradiol Acutely Potentiates Hippocampal Excitatory Synaptic Transmission through a Presynaptic Mechanism. *J. Neurosci.* **30**, 16137–16148 (2010).

37. J. Cao, J. Meitzen, Perinatal activation of ERα and ERβ but not GPER-1 masculinizes female rat caudate-putamen medium spiny neuron electrophysiological properties. *J. Neurophysiol.* **125**, 2322–2338 (2021).

38. H. A. Halem, J. A. Cherry, M. J. Baum, Vomeronasal neuroepithelium and forebrain Fos responses to male pheromones in male and female mice. *J. Neurobiol.* **39**, 249–263 (1999).

39. B. Yang, T. Karigo, D. J. Anderson, Transformations of neural representations in a social behaviour network. *Nature* **608**, 741–749 (2022).

40. Y. Hasegawa, *et al.*, Generation of CRISPR/Cas9-mediated bicistronic knock-in *ins1-cre* driver mice. *Exp. Anim.* **65**, 319–327 (2016).

41. M. C. Tsuda, S. Ogawa, Long-Lasting Consequences of Neonatal Maternal Separation on Social Behaviors in Ovariectomized Female Mice. *PLOS ONE* **7**, e33028 (2012).

42. O. Friard, M. Gamba, BORIS: a free, versatile open-source event-logging software for video/audio coding and live observations. *Methods Ecol. Evol.* **7**, 1325–1330 (2016).

43. A. Mathis, *et al.*, DeepLabCut: markerless pose estimation of user-defined body parts with deep learning. *Nat. Neurosci.* **21**, 1281–1289 (2018).

Figures

Figure 1. Fiber photometry recordings from MeApd-ERβ$^+$ neurons during sexual preference test

(A) Schematic diagram of AAV injection and fiber implantation in the MeApd.

(B) Schematic diagram of the fiber-photometry system used in this study (465 nm LED emission light, filter 525 nm).

(C) Representative photo (left) and schematic diagram of preference test setup(right).

(D) Duration of time (sec) spent in contact area during RF (Red) vs XF (Orange) preference tests (Mean ± SEM, n = 7, ***: p = 0.0004, Student's t-test).

(E) Sniffing duration (sec) towards each stimulus during RF (Red) vs XF (Orange) preference tests (Mean ± SEM, n = 7, ***: p = 0.0008, Student's t-test).

(F) Mean GCaMP7f signals (Z score) during sniffing towards RF (Red:150 events) and XF (Orange:134 events) stimulus mice. Data derived from 7 male mice and shown for 10 sec (2 s before to 8 s after) around the onset of each sniffing event.

(G) Mean peak GCaMP7f signals recorded from MeApd-ERβ$^+$ neurons during each sniffing event in RF (Red) vs XF (Orange) preference tests. Peak value represents the maximum Z score change within 8 s from sniffing onset. Activity data from 2 s before the onset of sniffing was used as baseline value. (Mean ± SEM, n = 7, ****: p < 0.00001, Student's t-test).

(H) Duration (sec) of time spent in the contact area during RF (Red) vs IM (Blue) preference tests (Mean ± SEM, n = 7, p = 0.0550, Student's t test).

(I) Sniffing duration (sec) towards each stimulus during RF (Red) vs IM (Blue) preference tests (Mean ± SEM, n = 7, ***: p = 0.0057, Student's t-test).

(J) Mean GCaMP7f signals (Z score) during sniffing towards RF (Red:150 events) and IM (Blue:170 events) stimulus mice. Data derived from 7 male mice and shown for 10 sec (2 s before to 8 s after) around the onset of each sniffing event.

(K) Mean peak GCaMP7f signals recorded from MeApd-ERβ$^+$ neurons during each sniffing event in RF (Red) vs vs IM (Blue) preference tests. Peak value represents the maximum Z score

change within 8 s from sniffing onset. Activity data from 2 s before the onset of sniffing was used as baseline value (Mean ± SEM, n = 7, *: p = 0.0104, Student's t-test).

Figure 2. Fiber photometry recordings from MeApd-ERβ$^+$ neurons towards individually presented social stimuli

(A) Duration of time spent in the contact area during RF (Red) vs Empty (Gray) preference tests (Mean ± SEM, n = 5, p = 0.0576, Student's t-test).

(B) Mean GCaMP7f signals (Z scored) during sniffing towards RF (Red:117 events) and Empty (Gray:121 events) cylinders. Data derived from 5 male mice and shown for 10sec (2 s before to 8 s after) around the onset of each sniffing event.

(C) Mean peak GCaMP7f signals recorded from MeApd-ERβ$^+$ neurons during each sniffing event in RF (Red) vs Empty (Gray) preference tests (Mean ± SEM, n = 5, *: p = 0.0123 Student's t-test).

(D) Duration of time(sec) spent in contact area during XF (Orange) vs Empty (Gray) preference tests (Mean ± SEM, n = 5, *: p = 0.0127, Student's t-test).

(E) Mean GCaMP7f signals (Z score) during sniffing towards XF (Orange:131 events) and Empty (Gray:124 events) cylinders. Data derived from 5 male mice and shown for 10 sec (2 s before to 8 s after) around the onset of each sniffing event.

(F) Mean peak GCaMP7f signals recorded from MeApd-ERβ$^+$ neurons during each sniffing event in XF (Orange) vs Empty (Gray) tests. (Mean ± SEM, n = 5, p = 0.0951, Student's t-test).

(G) Duration of time spent in the contact area(sec) during IM(Blue) vs Empty (Gray) tests (Mean ± SEM, n = 5, ***: p = 0.0005, Student's t-test).

(H) Mean GCaMP7f signals (Z score) during sniffing towards IM (Blue:130 events) and Empty (Gray: 114 events) cylinders. Data derived from 5 male mice and shown for 10 sec (2 s before to 8 s after) around the onset of each sniffing event.

(I) Mean peak GCaMP7f signals recorded from MeApd-ERβ$^+$ neurons during each sniffing event in IM (Blue) vs Empty (Gray) tests (Mean ± SEM, *, n = 5, p = 0.0123, Student's t-test).

Figure 3. DREADD inhibition of MeApd-ERβ$^+$ neurons disrupt receptivity-based, but not sex-based, preference in male mice

(A) Schematic diagram of bilateral AAV injection in the MeApd.

(B) Representative image showing expression of hM4Di-mCherry in MeApd-ERβ$^+$ neurons (scale = 500 um).

(C) Schematic diagram and timeline for preference tests with DREADD inhibition. Male mice were injected with AAV and tested for receptivity-based and sex-based preference in three consecutive days for each with either saline (day 1 and 3) or CNO (day 2; 1 mg/kg) injections.

(D) Right: Mean percent (%) of time spent in contact area of RF cylinder during RF vs XF tests for hM4Di (Red) and mCherry control (Blue) groups. Values obtained by dividing the RF duration by total duration time spent in contact area of RF and XF cylinders. hM4Di (Red) and mCherry control (Blue) (Mean ± SEM, n = 11 for hM4Di and n = 9 for mCherry control, ****: $p < 0.0001$, Bonferroni's test). Left: Schematic diagram of the receptivity-based (RF vs XF) preference test and representative heat map of body position in each test performed in three consecutive days. Data were obtained from a hM4Di injected animal.

(E) Right: Mean percent (%) time spent in contact area of RF cylinder during RF vs IM tests for hM4Di (Red) and mCherry control (Blue) groups. Values obtained by dividing RF duration by total duration of time spent in contact area of RF and IM cylinders. hM4Di (Red) and mCherry control (Blue) (Mean ± SEM, n = 11 for hM4Di and n = 9 for mCherry control, ns, Bonferroni's test). Left: Schematic diagram of sex-based (RF vs IM) preference test and representative heat map of body position in each test performed in three consecutive days. Data obtained from a hM4Di injected animal.

Figure 4. DREADD inhibition of MeApd-ERβ$^+$ neurons affect BNSTp neuronal activity

(A) Schematic diagram of experimental paradigm. BNSTp neuronal activity was recorded non-specifically with fiber photometry imaging system while MeApd-ERβ$^+$ neurons were inhibited.

(B) Schematic diagram of AAV injection. Non-specific GCaMP7f expressing virus was injected unilaterally in the BNST, and Cre dependent hM4Di expressing virus was injected bilaterally in MeApd.

(C) Representative image in the BNSTp expressing GCaMP7f (Green), projecting fibers from hM4Di expressing MeApd-ERβ$^+$ neurons (Red) and DAPI (Blue) in the MeApd (Scale bar = 500μm). White dots represent tracks from the inserted fiber.

(D) Mean GCaMP7f signals (Z score) during sniffing towards RF (Red:180 events) and XF (Orange:149 events) stimulus mice in saline injected control sessions. Data derived from 6 male mice and shown for 10 sec (2 s before to 8 s after) around onset of each sniffing event.

(E) Mean GCaMP7f signals (Z score) during sniffing towards RF (Red:151 events) and XF (Orange:154 events) stimulus mice in CNO injected sessions. Data derived from 6 male mice and shown for 10 sec (2 s before to 8 s after) around onset of each sniffing event.

(F) Mean peak GCaMP7f signals recorded from BNSTp neurons during each sniffing event in RF (Red) vs XF(Orange) tests. (Mean ± SEM, n = 6, ***: $p < 0.001$, Bonferroni's test).

(G) Mean GCaMP7f signals (Z scored) during sniffing towards RF (Red: 165 events) and IM (Blue: 174 events) stimulus mice in saline injected control sessions. Data derived from 6 male mice and shown for 10 sec (2 s before to 8 s after) around onset of each sniffing event.

(H) Mean GCaMP7f signals (Z score) during sniffing towards RF (Red: 156 events) and IM (Blue:142 events) stimulus mice in CNO injected sessions. Data derived from 6 male mice and shown for 10 sec (2 s before to 8 s after) around onset of each sniffing event.

(I) Mean peak GCaMP7f signals recorded from BNSTp neurons during each sniffing event in RF (Red) vs IM (Blue) tests. (Mean ± SEM, n = 6, ***: $p < 0.001$, Bonferroni's test).

Figure 5. Schematic summary of MeApd-ERβ$^+$ neuron function

(A) Schematic diagram of function of MeApd-ERβ$^+$ neurons during receptivity-based (RF vs XF) preference tests. Sniffing towards RF induces excitation of MeApd-ERβ$^+$ neurons, which further accentuates approach and sniffing to RF. Neuronal activity of MeApd-ERβ$^+$ neurons, in turn, affects downstream BNSTp neuronal activity during receptivity-based preference test to fully promote receptivity-based preference.

(B) Schematic diagram of function of MeApd-ERβ$^+$ neurons during sex-based (RF vs IM) preference tests. Although MeApd-ERβ$^+$ neurons respond more to RF in RF vs IM preference test, MeApd-ERβ$^+$ neuronal activity, per se, is not necessary for expression of preference to RF over IM. Differential responses of BNSTp neurons during sniffing of RF and IM are maintained without input signal from MeApd-ERβ$^+$ neurons.

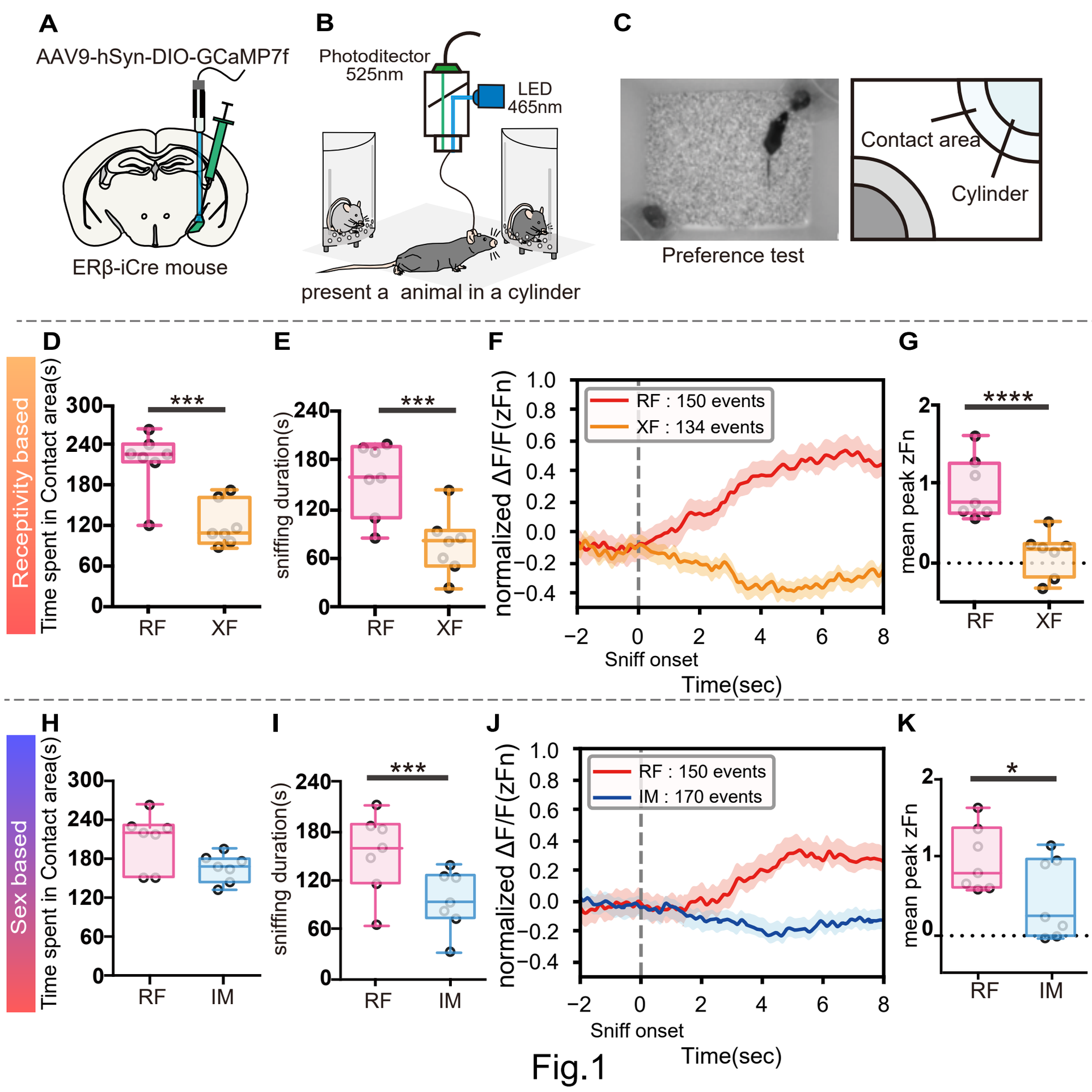
A
AAV9-hSyn-DIO-GCaMP7f
ERβ-iCre mouse
B
Photoditector
525nm
LED
465nm
present a animal in a cylinder
C
Contact area
Cylinder
Preference test
Receptivity based
D
Time spent in Contact area(s)
***
RF
XF
E
sniffing duration(s)
***
RF
XF
F
normalized ΔF/F(zFn)
RF : 150 events
XF : 134 events
Sniff onset
Time(sec)
G
mean peak zFn
****
RF
XF
Sex based
H
Time spent in Contact area(s)
RF
IM
I
sniffing duration(s)
***
RF
IM
J
normalized ΔF/F(zFn)
RF : 150 events
IM : 170 events
Sniff onset
Time(sec)
K
mean peak zFn
*
RF
IM

Fig.1

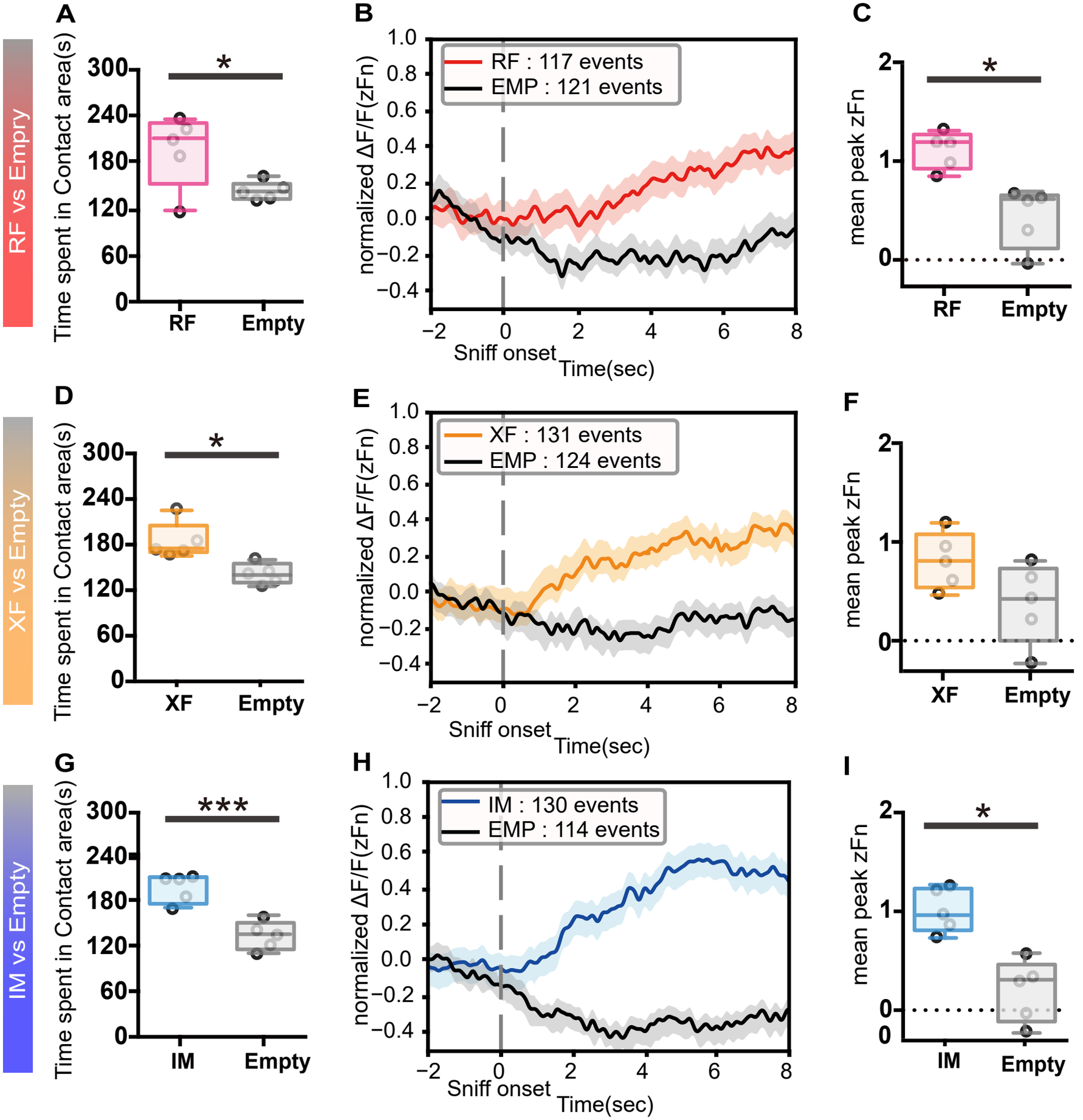
RF vs Empry
XF vs Empty
IM vs Empty
A
B
C
D
E
F
G
H
I
Time spent in Contact area(s)
300
240
180
120
60
0
*
RF
Empty
normalized ΔF/F(zFn)
RF : 117 events
EMP : 121 events
1.0
0.8
0.6
0.4
0.2
0.0
−0.2
−0.4
−2
0
2
4
6
8
Sniff onset
Time(sec)
mean peak zFn
2
1
0
XF : 131 events
EMP : 124 events
XF
IM : 130 events
EMP : 114 events
IM
***

Fig.2

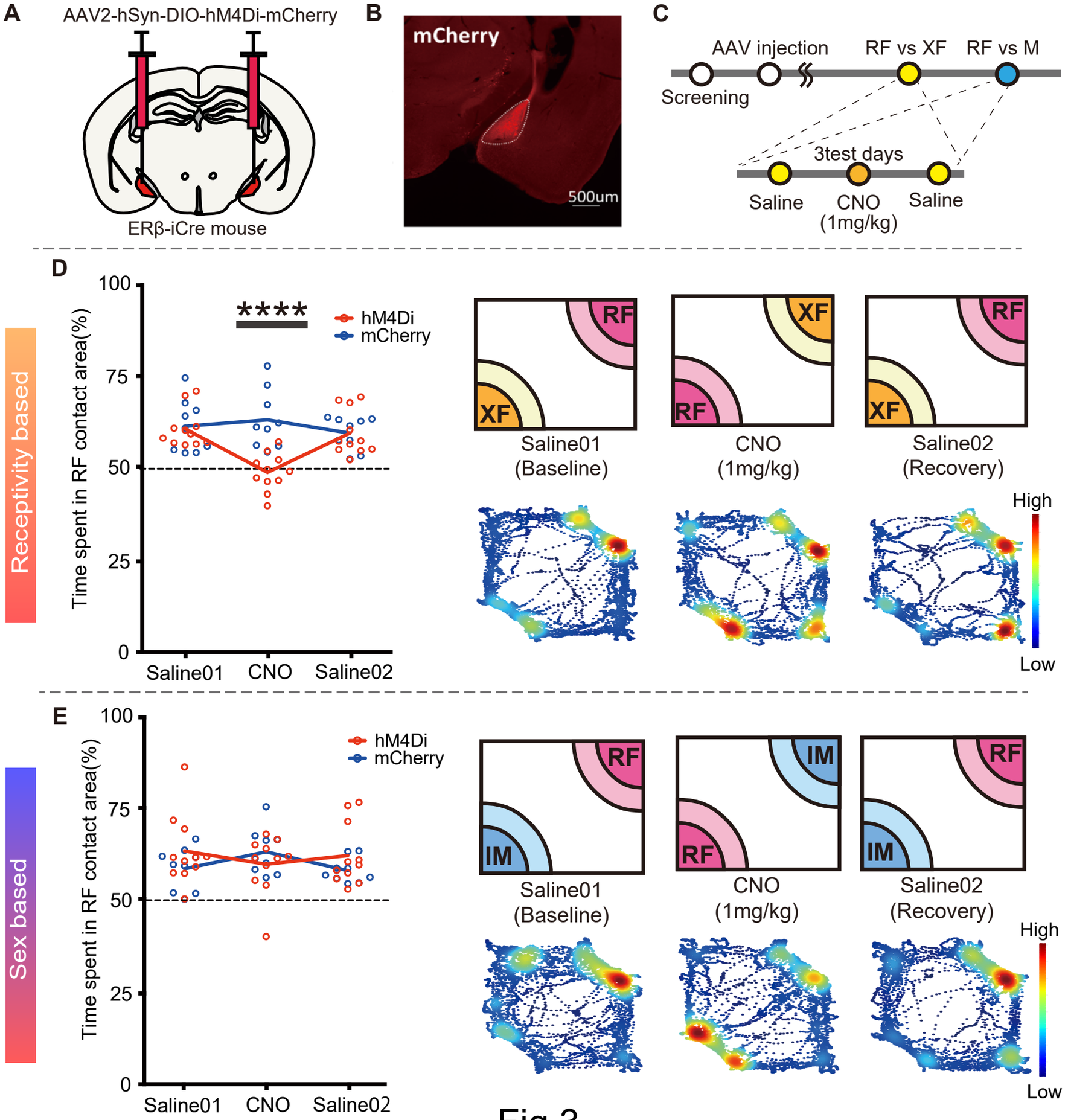
A
AAV2-hSyn-DIO-hM4Di-mCherry
ERβ-iCre mouse
B
mCherry
500um
C
AAV injection
RF vs XF
RF vs M
Screening
3test days
Saline
CNO
(1mg/kg)
Saline
D
Receptivity based
Time spent in RF contact area(%)
****
hM4Di
mCherry
Saline01
CNO
Saline02
RF
XF
Saline01
(Baseline)
CNO
(1mg/kg)
Saline02
(Recovery)
High
Low
E
Sex based
Time spent in RF contact area(%)
hM4Di
mCherry
Saline01
CNO
Saline02
RF
IM
Saline01
(Baseline)
CNO
(1mg/kg)
Saline02
(Recovery)
High
Low

Fig.3

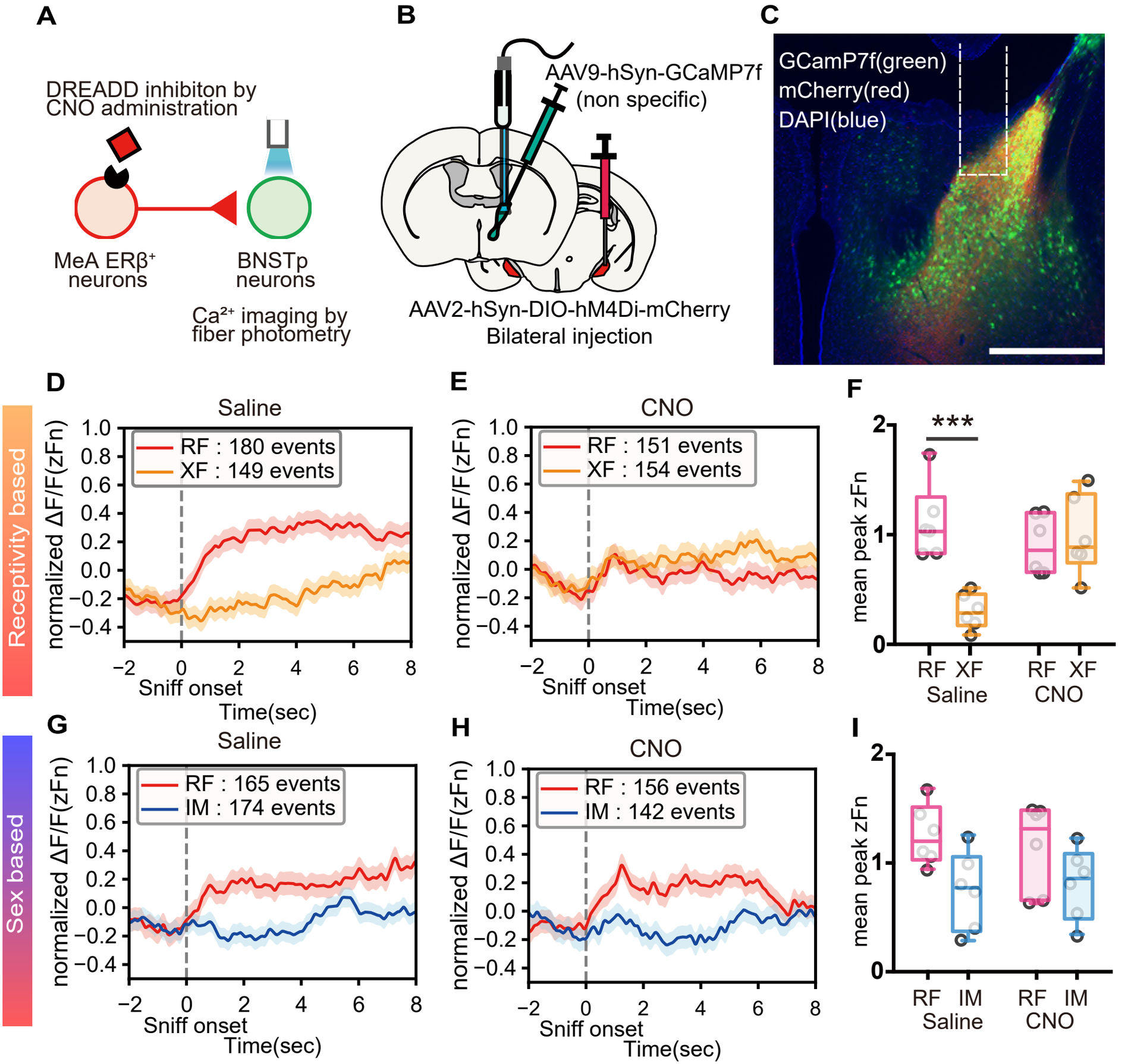
A
DREADD inhibiton by
CNO administration
MeA ERβ+
neurons
BNSTp
neurons
Ca2+ imaging by
fiber photometry
B
AAV9-hSyn-GCaMP7f
(non specific)
AAV2-hSyn-DIO-hM4Di-mCherry
Bilateral injection
C
GCamP7f(green)
mCherry(red)
DAPI(blue)
Receptivity based
D
Saline
RF : 180 events
XF : 149 events
normalized ΔF/F(zFn)
Sniff onset
Time(sec)
E
CNO
RF : 151 events
XF : 154 events
F
***
mean peak zFn
RF XF
Saline
RF XF
CNO
Sex based
G
Saline
RF : 165 events
IM : 174 events
H
CNO
RF : 156 events
IM : 142 events
I
RF IM
Saline
RF IM
CNO

Fig.4

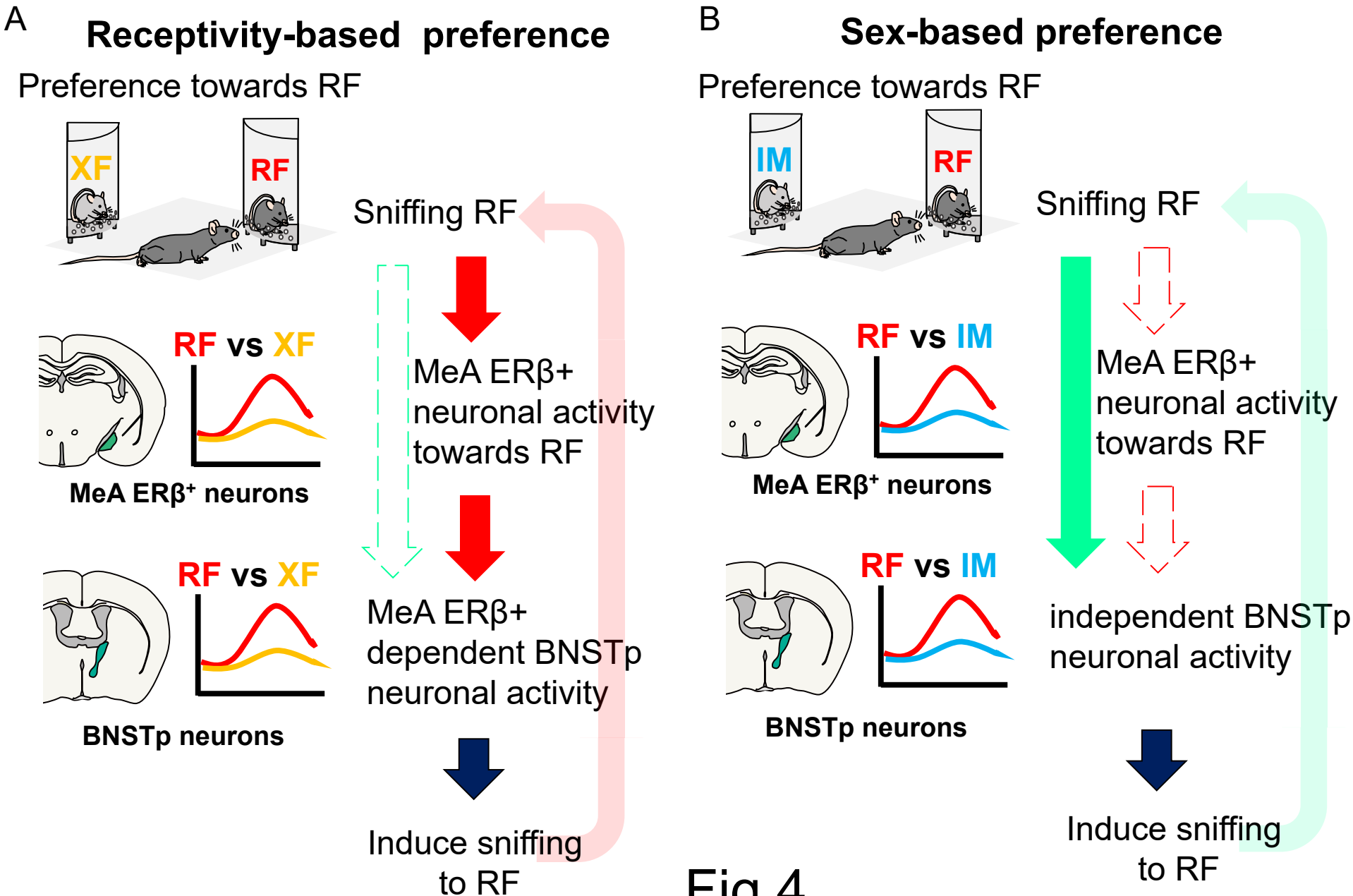
A
Receptivity-based preference
Preference towards RF
XF
RF
Sniffing RF
RF vs XF
MeA ERβ+ neuronal activity towards RF
MeA ERβ⁺ neurons
RF vs XF
MeA ERβ+ dependent BNSTp neuronal activity
BNSTp neurons
Induce sniffing to RF
B
Sex-based preference
Preference towards RF
IM
RF
Sniffing RF
RF vs IM
MeA ERβ+ neuronal activity towards RF
MeA ERβ⁺ neurons
RF vs IM
independent BNSTp neuronal activity
BNSTp neurons
Induce sniffing to RF

Fig.4